FEBS Letters 586 (2012) 3681–3691

FEBS Letters

journal homepage: www.FEBSLetters.org

Constitutive autotaxin transcription by Nmyc-amplified and non-amplified neuroblastoma cells is regulated by a novel AP-1 and SP-mediated mechanism and abrogated by curcumin

Antonietta R. Farina [a,1], Lucia Cappabianca [a,1], Pierdomenico Ruggeri [a], Natalia Di Ianni [a], Marzia Ragone [a], Stefania Merolle [a], Kimihiko Sano [b], Mary L. Stracke [c], Jonathan M. Horowitz [d], Alberto Gulino [e], Andrew R. Mackay [a,*]

[a] Section of Molecular Pathology, Department of Experimental Medicine, University of L'Aquila, 67100 L'Aquila, Italy
[b] Department of Pediatrics, Kobe University School of Medicine, Kobe 650, Japan
[c] Laboratory of Pathology, NCI, NIH, Bethesda, MD 20892, USA
[d] Department of Anatomy, Physiological Sciences and Radiology, North Carolina State University, Raleigh, NC 27606, USA
[e] Department of Experimental Medicine and Pathology, University of Rome "La Sapienza", 00161 Rome, Italy

ARTICLE INFO

Article history:
Received 29 June 2012
Revised 11 August 2012
Accepted 24 August 2012
Available online 6 September 2012

Edited by Ivan Sadowski

Keywords:
Autotaxin
Transcription
Neuroblastoma
AP-1
SP
Internally initiated SP3
Curcumin

ABSTRACT

The motility, angiogenesis and metastasis-stimulating factor Autotaxin (Atx), over expressed by human neuroblastomas (NB), is constitutively expressed by human Nmyc-amplified SK-N-BE and non-Nmyc-amplified SH-SY5Y NB cells. Here, we characterise a novel Atx transcriptional mechanism, utilised by both cell lines, that is restricted to the first 285 bp of the *Atx* promoter and involves AP-1 and SP transcription factors, acting through a CRE/AP-1-like element at position −142 to −149 and a GAbox at position −227 to −235 relative to the Atx translational start site. This novel transcriptional mechanism can be inhibited by internally initiated SP-3 and the natural phenol curcumin.

1. Introduction

Autotaxin (Atx), originally identified as an autocrine motility factor in melanoma cells [1–3], catalyses the transformation of lysophosphatidyl choline into lysophosphatidic acid (LPA) and forms an Atx/LPA/LPA receptor axis that promotes tumour progression by modulating cancer-related inflammation; inhibiting apoptosis; stimulating angiogenesis, tumour cell motility, invasion and metastasis; and promoting metastatic bone disease by activating osteoclasts [4–11]. Atx overexpression has been implicated in the progression of breast, ovary, thyroid, liver, kidney and lung malignancies and nervous system tumours glioblastoma and neuroblastoma (NB) [5,6,11–20]. Atx is, therefore, considered a novel cancer therapeutic target.

NB is an aggressive tumour that arises during sympathetic nervous system development from neural crest cells of the sympathoadrenal lineage and accounts for approximately 10% of all paediatric tumours [21,22]. Despite general therapeutic improvements, the age of onset and high frequency of post-therapeutic relapse translate into low survival rates, highlighting the need for greater understanding of the molecular mechanisms involved in NB pathogenesis and progression and translation into novel therapeutic strategies. NBs are highly heterogeneous and exhibit a high degree of genetic and biological variability. Advanced stage NBs metastasise to bone, bone marrow, lymph nodes, liver and skin, with metastatic bone disease carrying the poorest prognosis. Amplification of the Nmyc gene characterises a significant proportion of aggressive NBs and has been implicated in Atx expression [20,21].

In spite of the role played by the Atx/LPA/LPA receptor axis in tumour progression, relatively little is known about the transcrip-

Abbreviations: Atx, autotaxin; NB, neuroblastoma; CRE, cAMP response element; CREB, CRE binding protein; ATF, activating transcription factor; GAPDH, glyceraldehyde-3-phosphate dehydrogenase; EMSA, electro-mobility shift assay; ChIp, chromatin immunoprecipitation; AP1, activator protein-1; SP, specificity protein

* Corresponding author. Fax: +39 0862433523.
E-mail address: andrewreay.mackay@univaq.it (A.R. Mackay).

[1] The first two authors contributed equally to this work.

0014-5793/$36.00
http://dx.doi.org/10.1016/j.febslet.2012.08.026

tional regulation of Atx. The human Atx promoter has been cloned and characterised as containing several putative SP sites but no typical TATA or CAAT boxes. Atx transcription initiates from bases −61 and −64, relative to the translational start site (+1) [20,23] and in human NB cells has been attributed to Nmyc acting through a putative myc element within an uncharacterised 33 bp promoter region (−287 to −254), which also contains a putative GATA element [20], or to be regulated by retinoic acid in Nmyc amplified NB cells in an Nmyc-independent manner [24]. In human breast cancer cells, α6β4 integrin receptor activation stimulates Atx transcription through putative NFAT sites at positions −310 and −1780 [25] and Atx transcriptional repression has been attributed to histone de-acetylases HDAC3 and HDAC7 [26]. In chick embryo fibroblasts v-Jun oncogene induces Atx expression [27], whereas in murine embryonic fibroblasts HOXA group 13 transcription factors have been implicated in Atx expression [28].

Here, we report a novel Nmyc-independent transcriptional mechanism for Atx expression, utilised by both Nmyc amplified and non-amplified NB cells, that involves AP-1 and SP transcription factors acting through CRE/AP-1-like and GAbox within the first 285 bp of the Atx promoter and can be inhibited by internally initiated SP-3 and curcumin.

2. Materials and methods

2.1. Cells and reagents

Cell lines, reagents and culture conditions are described in Supplementary material.

2.2. Nuclear extracts

Nuclear extracts were prepared as previously described [29]. Protein concentrations were determined by Bio-Rad assay, as directed by the manufacturer (Bio-Rad, Hercules, CA).

2.3. In vitro footprinting

In vitro footprint analysis was performed as previously reported [30], and is described in Supplementary material.

2.4. Electrophoretic mobility shift assays (EMSAs)

EMSAs were performed as previously described [31]. The Atx-specific oligonucleotide sequences are provided in Supplementary material.

2.5. Plasmid constructs

The Atx reporter gene constructs −1197Atx and −287Atx have been previously reported [20]. All other Atx reporter gene deletion and mutated constructs are described in Supplementary material.

2.6. Transient transfection and reporter gene assays

Cells grown on 60 mm petri dishes were transfected with supercoiled plasmid DNA (3 μg) using Lipofectamine™, as directed (Invitrogen, Carlsbad, CA). Conditions and reporter gene assays are described in Supplementary material.

2.7. Chromatin immunoprecipitation assays (ChIp)

ChIp assays were performed as previously described [32]. The oligonucleotide sequences used are detailed in Supplementary material.

2.8. Immunoblotting

Western blots were performed as previously described [33], using either 50–100 μg of nuclear extracts or 20-fold concentrated 72 h serum-free culture conditioned medium for Atx. Coomassie blue-stained membranes were used to control differences in loading. Densitometric analyses were performed using Molecular Analysis Software for the BioRad 710 Imaging densitometer.

2.9. RT-PCR analysis of Atx expression in NB cells

RT reactions were performed on total RNAs (1 μg) using the Moloney Murine Leukaemia virus RT kit, as detailed by the manufacturer (Life Technologies, Inc., Paisley, UK). RT reactions were subjected to PCR using the primers and conditions described in Supplementary material. Densitometric analysis of ethidium bromide stained RT-PCR products, separated by agarose gel electrophoresis, was performed using Molecular Analysis Software for the BioRad 710 Imaging densitometer.

2.10. Curcumin treatment

Sub-confluent (80% confluent) cell cultures were incubated with curcumin at the concentrations stated for 24 h, at 37 °C. Following incubation, non-adherent non-viable cells were removed by washing 3 times in pre-warmed PBS and total RNA extracted from the remaining viable adherent cell population, for RT-PCR comparison.

2.11. Statistical analysis

The Student's *t* test was used for statistical comparisons, means giving *t* values with associated probabilities of $\leqslant 0.05$ were considered statistically significant.

3. Results

3.1. SK-N-BE and SH-SY5Y cells express Atx

RT-PCR detected similar levels of Atx relative to GAPDH mRNA expression in Nmyc-amplified SK-N-BE and non-Nmyc-amplified SH-SY5Y cells, quantified by densitometric analysis of ethidium bromide stained gels as 63% and 58% of GAPDH levels, respectively (Fig 1A). Western blotting also detected similar levels of Atx protein in concentrated 72 h serum-free supernatants from identical cell numbers of SK-N-BE and SH-SY5Y cells. Densitometric quantification of Westerns, adjusted for differences in loading obtained by densitometric analysis of the Coomassie blue-stained membrane, indicated that SH-SY5Y cells had secreted 85% of the Atx levels secreted by an identical number of SK-N-BE cells (Fig 1B). Similar levels of Atx mRNA and protein expression characterised both sub confluent (80%) and confluent (100%) SH-SY5Y and SK-N-BE cell cultures (data not displayed).

3.2. The Atx promoter reporter gene is activated constitutively in SK-N-BE and SH-SY5Y cells

For Atx promoter sequence numeration, the A of the initiating codon ATG is defined as +1, as previously described [20].

SK-N-BE and SH-SY5Y cells constitutively activated a luciferase reporter gene construct containing 1197 bp of 5′ promoter sequence (−1197Atx) to similar non-statistically different levels ($P \leqslant 0.5$, $n = 18$). Promoter activity in both cell lines approximated to 10 000 RLUs/100 μg of protein extract. This is the equivalent of 10 pg of purified luciferase and represented a statistically signifi-

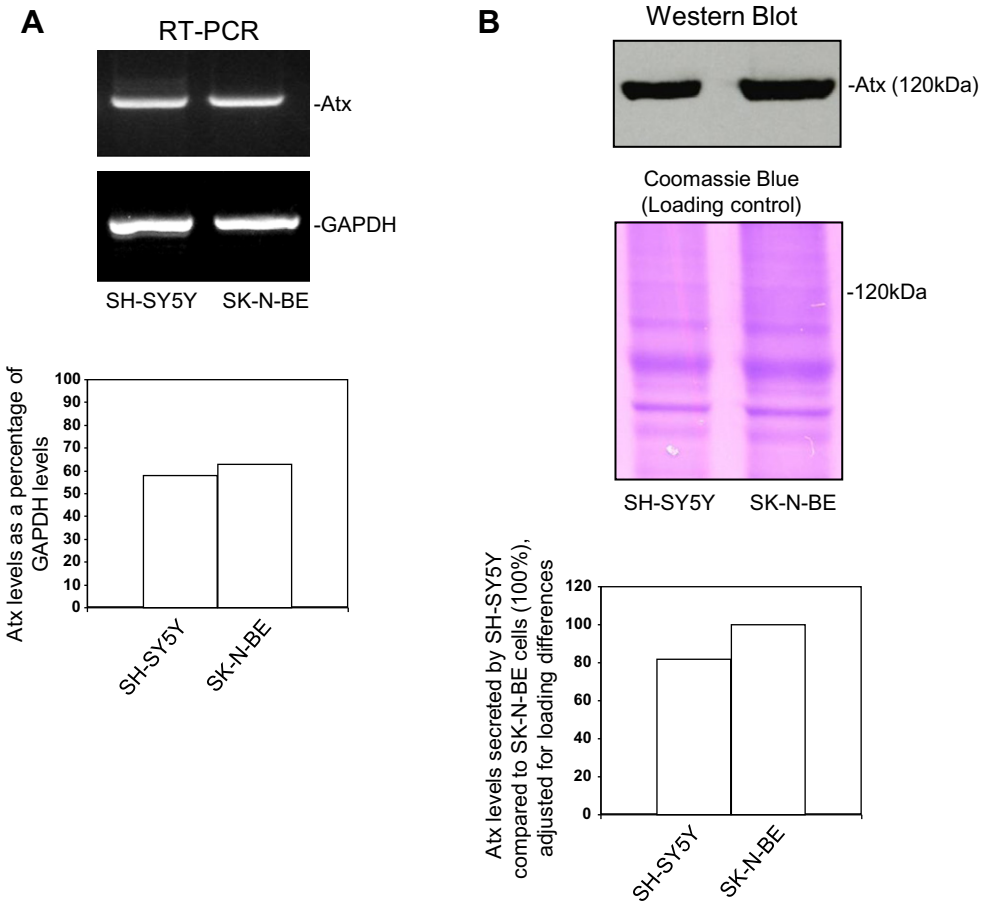

Fig. 1. Atx is expression by human NB cells. (A) Ethidium bromide-stained agarose gel demonstrating Atx and GAPDH RT-PCR products from exponentially growing SH-SY5Y and SK-N-BE cells plus a histogram demonstrating densitometric quantification of Atx RT-PCR levels in SK-N-BE and SH-SY5Y cells, expressed as a percentage of GADH levels in the adjacent gel. (B) A representative Western blot demonstrating levels of 120 kDa Atx in 20-fold concentrated 72 h serum-free conditioned medium from identical numbers of SH-SY5Y and SK-N-BE cells (upper panel), the Coomassie blue-stained membrane as a loading control (middle panel) and a histogram demonstrating densitometric quantification of Atx proteins levels secreted by SH-SY5Y cells as a percentage of Atx levels secreted by an equal number of SK-N-BE cells, in the adjacent Western blot, given the arbitrary value of 100%, adjusted for differences in protein loading obtained by densitometric analysis of the Coomassie blue-stained membrane.

cant increase in activity of >100 fold over the basic promoter-less construct PGL_2 (100 RLU/100 μg protein) ($P < 0.001$, $n = 18$) (Fig. 2A). The deletion of 912 bp of 5′ upstream Atx sequence to give the construct −285Atx, did not significantly reduce reporter gene activity in either SK-N-BE or SH-SY5Y cells ($P \leqslant 0.5$ for both cell lines, $n = 18$). A further 150 bp deletion to give the construct −135Atx, significantly reduced Atx promoter activity by <95% in both SH-SY5Y and SK-N-BE cells ($P \leqslant 0.001$, $n = 18$, for both cell lines) (Fig 2A).

3.3. In vitro footprint analysis of the Atx promoter in SK-N-BE and SH-SY5Y cells

DNAse In vitro footprinting of the Atx promoter region from −317 to −26 identified two identical areas protected by SK-N-BE and SH-SY5Y nuclear extracts. The first, bases −155 to −137 (5′-CCTGTGATGTAATCAAGCT-3′), contains a CRE/AP-1-like site (underlined) and the second, bases −238 to −207 (5′-TTAGGGGAGGGACCTGTAAGGGGCGGGGATAA-3′), contains a GAbox and a GCbox (underlined) (Fig. 2B).

3.4. Atx-promoter deletion and mutation analysis

Deletion of 71 bp from the construct −285Atx to give the construct −214Atx, eliminating putative myc, GATA and GA elements, significantly reduced luciferase activity in SK-N-BE (Fig 3A) and SH-SY5Y (Fig 3B) cells by approximately 50% ($P \leqslant 0.001$, $n = 18$ for both cell lines). Further deletions of 10 bp (−204Atx), eliminating the GCbox, 12 bp (−182Atx), 20 bp (−162Atx) and 6 bp (−156Atx) did not further reduce promoter activity below that detected using the −214Atx construct in SK-N-BE cells (Fig. 3A, all deletions) or SH-SY5Y cells (Fig 3B, −156Atx only). Elimination of the CRE/AP-1-like element by a further 11 bp deletion (−145Atx, SK-N-BE cells) or a further 21 bp deletion (−135Atx, SH-SY5Y and SK-N-BE cells) reduced promoter activity by >95%, compared to the intact promoter ($P \leqslant 0.001$, $n = 18$ for both cell lines) (Fig. 3A and B).

Within the context of the full promoter, GAbox mutation from 5′-GGGGAGGG-3′ to 5′-G*c*GG*cc*G*c*-3′ (−1197GAm) significantly reduced promoter activity by 52 ± 7.5% in SK-N-BE cells (Fig. 3A) and 50 ± 6.8% in SH-SY5Y cells (Fig. 3B) ($P \leqslant 0.001$ for both cell lines). GCbox mutation from 5′-GGGGCGGGG-3′ to 5′-G*a*G*atc*GGG-3′ (−1197GCm) did not reduce activity in either cell line (Fig. 3A and B). CRE/AP-1-like site mutation from 5′-TGATGTAAT-3′ to 5′-T*tt*T*t*T*cc*T-3′ (−1197CRE/AP-1 m) significantly reduced activity by 55 ± 9.5% in SK-N-BE cells (Fig. 3A) and by 61 ± 8.5% in SH-SY5Y cells (Fig. 3B) ($P \leqslant 0.001$, for both cell lines). Combined GAbox and CRE/AP-1-like site mutation (−1197GAmCREm) significantly reduced activity by >90% in both cell lines (Fig. 3A and B) ($P \leqslant 0.001$, for both cell lines). Neither Myc site (−260) mutation from 5′-CACATGA-3′ to 5′-CA*ggcct*-3′ (−1197Mycm, both SK-N-BE

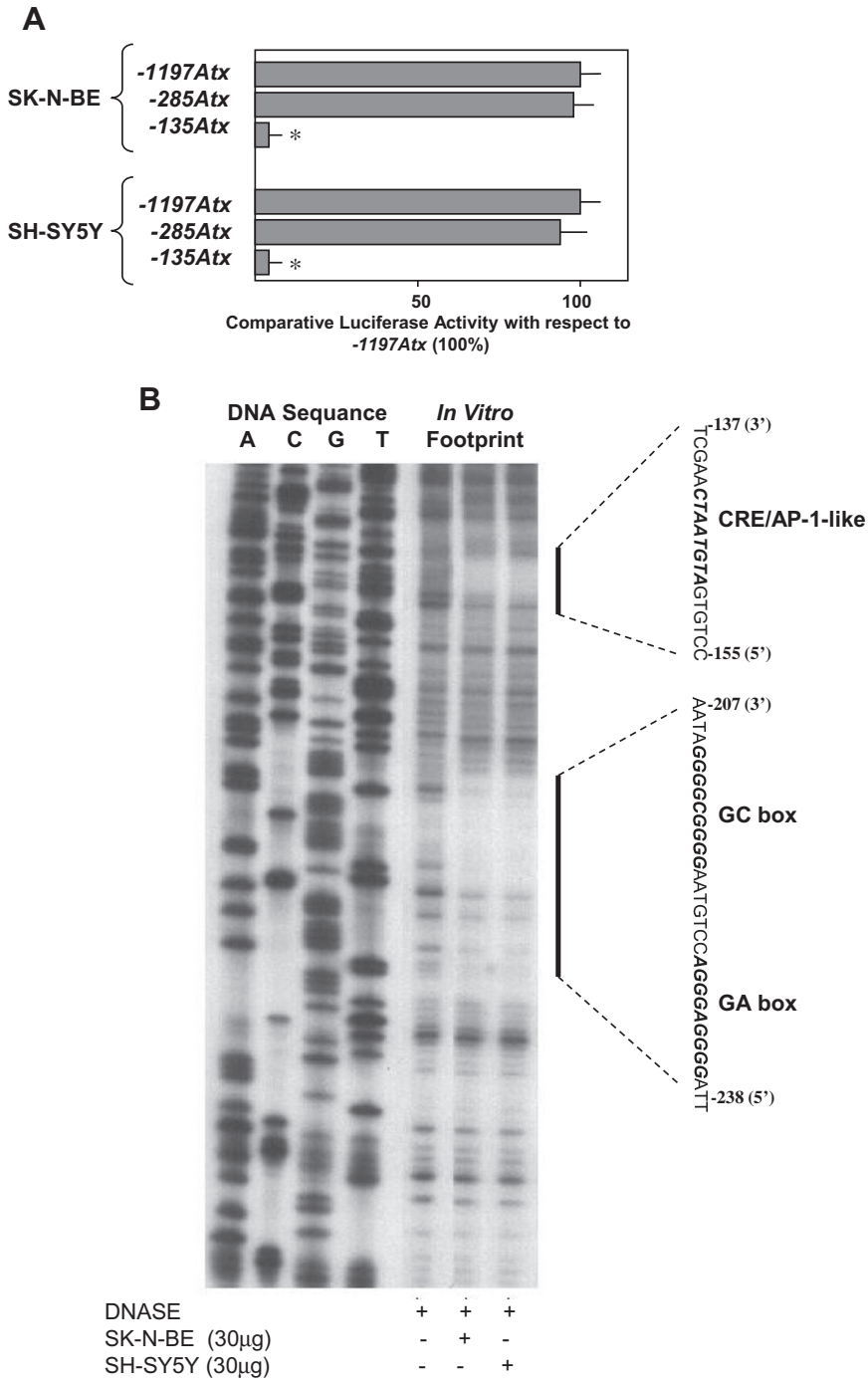

Fig. 2. In vitro footprint analysis. (A) Histogram comparing the percentage difference in −1197Atx, −285Atx and −135Atx reporter gene activity in SK-N-BE and SH-SY5Y cells. Results are displayed as percentage luciferase activity with respect to −1197Atx (100%) in 3 independent experiments, performed in triplicate (* = significant difference). (B) In vitro footprint demonstrating two areas protected by SK-N-BE and SH-SY5Y nuclear extracts (30 µg) within the Atx promoter region −317 to −26 (lanes 1–4 promoter DNA sequence). DNAse protected regions (lanes 6 and 7) exhibit a difference in banded appearance compared to the promoter digested by DNAse (+) in the presence of BSA (30 µg) (lane 5). Lines highlight protected regions. DNA sequences and position relative to the first A of the initiating codon ATG (+1) (translational start site), are provided.

and SH-SY5Y cells) nor GATA (−263) mutation from 5′-GGATAC-3′ to 5′-GG*cct*C-3′ (−1197GATAm, SK-N-BE cells only) reduced promoter activity (Fig. 3A and B).

Oligonucleotides bearing the above mutations did not bind specific proteins in SK-N-BE or SH-SY5Y nuclear extracts (not displayed). Mutated GAbox and CRE/AP-1-like oligonucleotides did not compete with specific GAbox and CRE/AP-1 like site binding complexes in nuclear extracts (Figs. 4B and 5B).

3.5. GAbox and CRE/AP-1-like site-binding complexes

The specificity of GAbox (Fig. 4A left panel SK-N-BE and Fig. 4B first 4 lanes SH-SY5Y) and CRE/AP-1-like (Fig. 5A left panel SK-N-BE and Fig. 5B left panel SH-SY5Y) site-binding complexes was confirmed by competition EMSA in which excess unlabelled specific but not non-specific (NS) or mutated oligonucleotides competed with complexes.

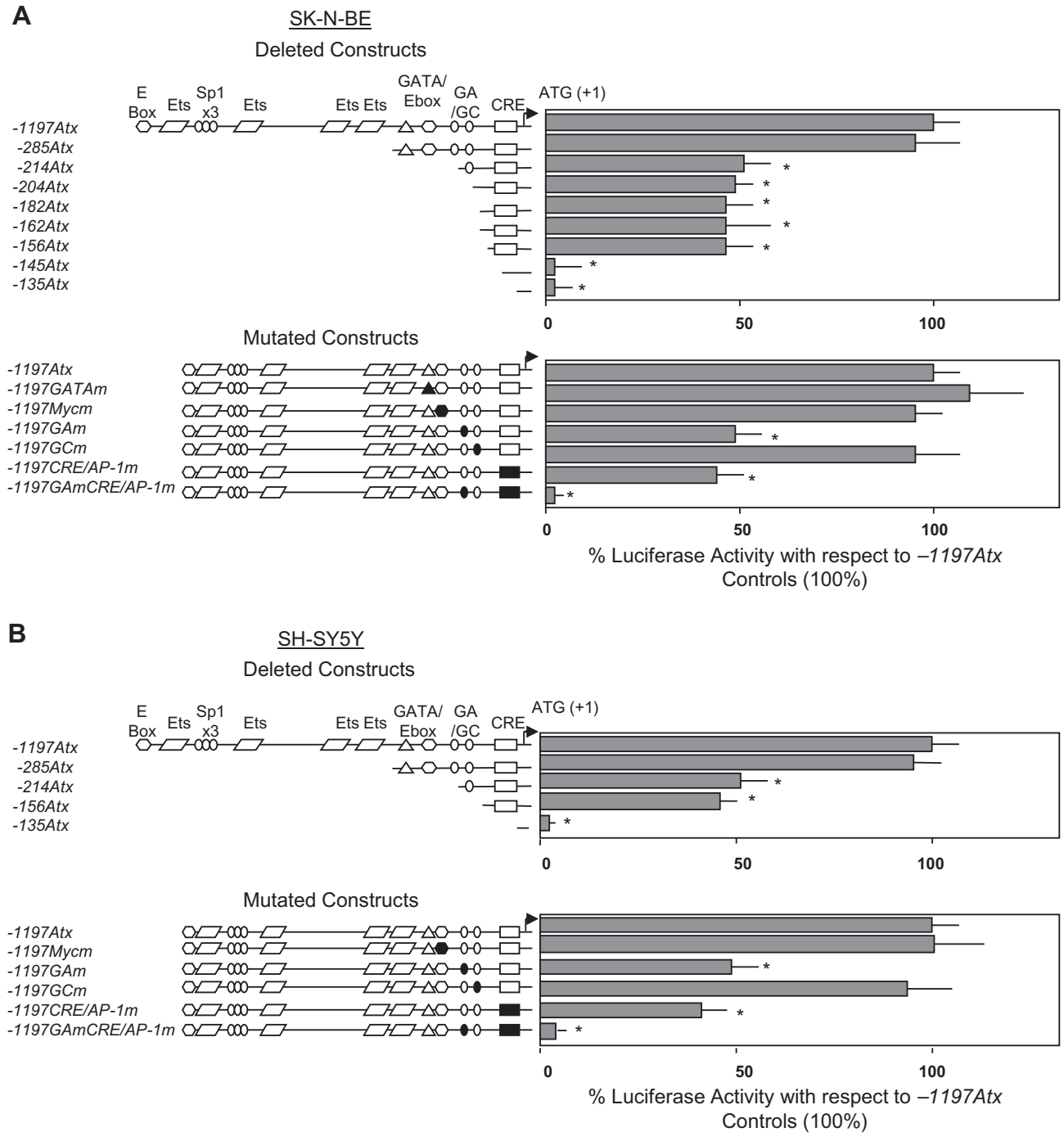

Fig. 3. Atx promoter reporter gene assays. Histograms depicting the percentage difference in luciferase activity in total cell extracts (100–200 μg protein) from (A) SK-N-BE and (B) SH-SY5Y cells transiently transfected with intact, deleted and point mutated Atx promoter reporter gene constructs, as indicated (left). Results are expressed as the mean (±s.e.) percentage difference in luciferase activity with respect to intact −1197Atx promoter controls (100%), in a minimum of 3 independent experiments performed in triplicate. Results were adjusted for differences in transfection efficiency determined by β-galactosidase assay. (Mutated elements are filled-in; arrows indicate the translational start site +1; * = significant difference).

Super-shift EMSA identified SP-1, SP-2 and SP-3 proteins in specific GAbox binding complexes (Fig. 4A right panel SK-N-BE and Fig. 4B last 5 lanes SH-SY5Y) and identified cjun, JunD, cfos, CREB-1 and ATF-1 proteins in specific CRE/AP-1-like site binding complexes (Fig. 5A right panel SK-N-BE, Fig. 5B right panel SH-SY5Y and Fig. 5C right panel SK-N-BE and left panel SH-SY5Y) in both cell lines. Western blots confirmed the presence of 65–80 kDa internally initiated SP-3 [34], in addition to 125–130 kDa full-length SP-3, 105 kDa SP-1, 85 kDa SP-2 and 105–110kda SP-4 proteins in nuclear extracts from both cell lines. Histone 4 levels are provided as an internal control for nuclear extracts (Fig. 4C). Variability in non-specific complex binding levels in competition EMSAs (Fig. 4A and B) most likely reflects competition of non-specific binding complexes by 100 fold excess competitor oligonucleotide and does not detract

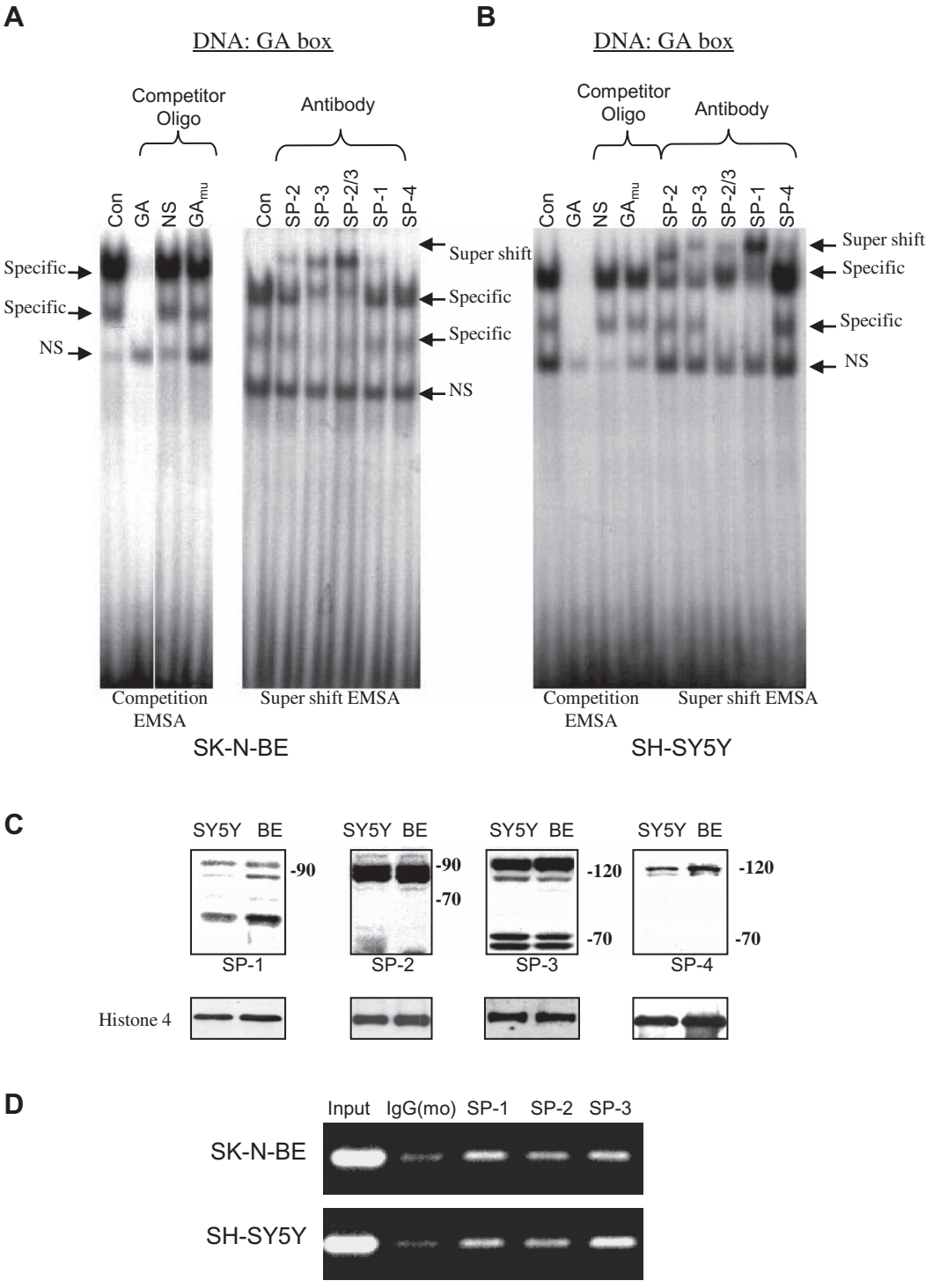

Fig. 4. GAbox binding complexes. Regular, competition and super-shift EMSAs demonstrating GAbox binding complex specificity (competiton EMSA) and protein content (super shift EMSA) in nuclear extracts from SK-N-BE cells (A) and SH-SY5Y cells (B). In Competition EMSAs, ^{32}P-labelled GA oligonucleotide probes were incubated with 100 fold excess unlabelled GAbox (GA), non-specific (NS) or mutated GAbox (GAmu) oligonucleotide competitors. In super shift EMSAs, binding reactions were incubated with anti-SP-1, SP-2, SP-3 or SP-4 antibodies (SP-1–4) (Specific, super shifted and non-specific (NS) binding complexes are indicated by arrows). (C) Western blots demonstrating SP-1, SP-2, SP-3, SP-4 and Histone 4 (internal control) protein levels in SK-N-BE and SH-SY5Y nuclear extracts (80 μg/lane). (D) ChIp detection of SP-1, SP-2 and SP-3 at the GA/GC box region of the endogenous Atx promoter in SK-N-BE and SH-SY5Y cells. Input material (Input) and pre-immune mouse IgG controls (mo), are provided.

from the clear demonstration that specific but not non-specific or mutated oligonucleotides competed with specific GA box binding complexes in competition EMSAs.

The GCbox (−219) oligonucleotide also bound specific complexes containing SP-1, SP-2 and SP-3 (data not displayed). Super-shift antibodies did not bind oligonucleotides in the absence of nuclear extracts.

3.6. Chromatin Immunoprecipitation (ChIp)

ChIp detected SP-1, SP-2 and SP-3 at the GA/GC box region (Fig. 4D) and detected cjun, JunD, CREB and ATF-1 at the CRE/AP-1 like site region (Fig. 5D) of the endogenous Atx promoter in both SK-N-BE and SH-SY5Y cells but, due to background problems, failed to conclusively demonstrate the presence of c-fos.

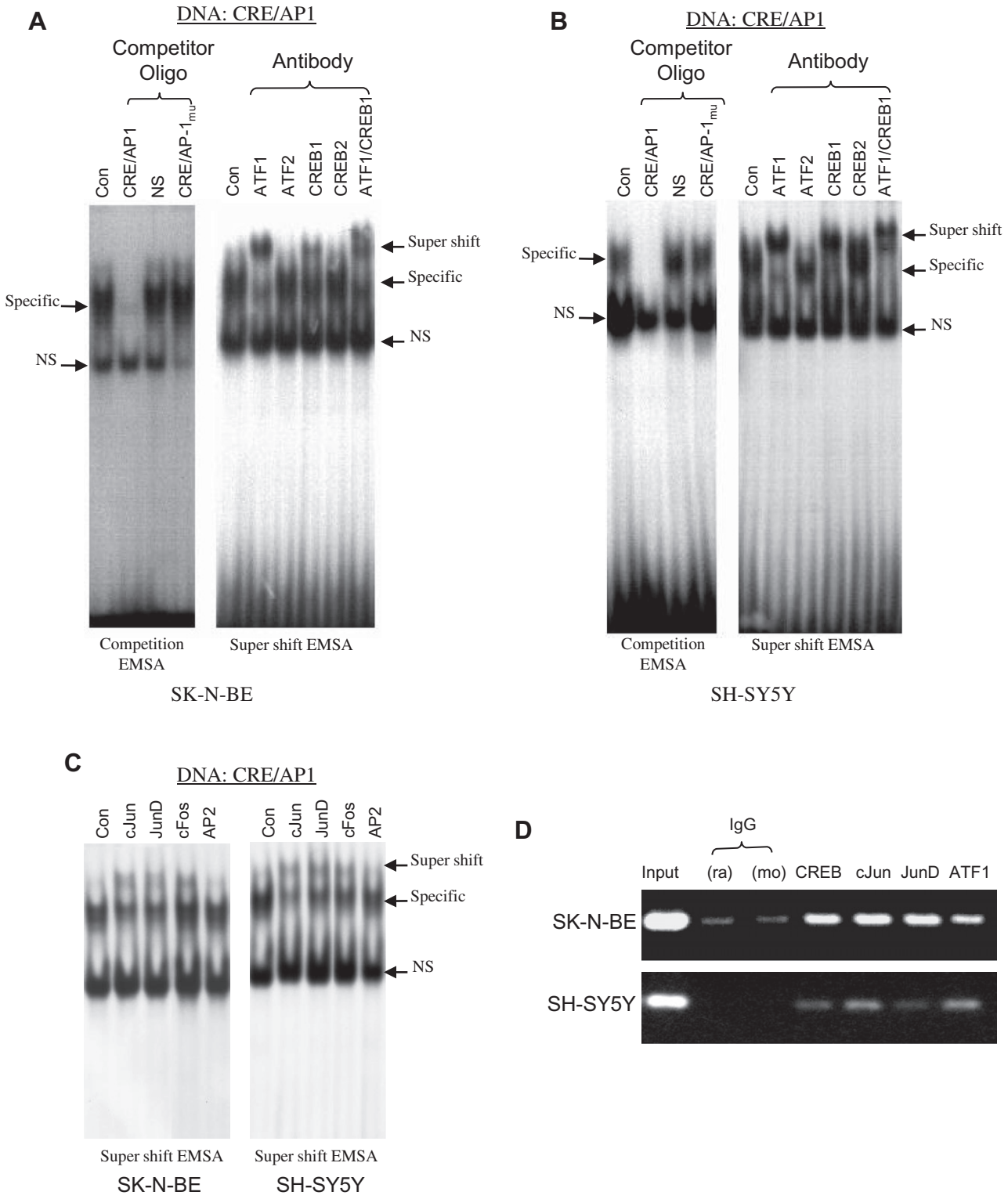

Fig. 5. CRE-AP-1-like site binding complexes. Regular, competition and super shift EMSAs demonstrating CRE/AP-1 like (−153) binding complex specificity (competition EMSA) and protein content (super shift EMSA) in nuclear extracts from SK-N-BE cells (A and C) and SH-SY5Y cells (B and C). In Competition EMSAs, ^{32}P-labelled CRE/AP-1 oligonucleotide probes were incubated with 100-fold excess unlabelled CRE/AP-1-like site, non-specific (NS) or mutated CRE/AP-1-like site (CRE/AP-1mu) oligonucleotide competitors. In super shift EMSAs, binding reactions were incubated with anti-CREB1, CREB2, ATF1, ATF2, cjun, junD, cfos or AP2 antibodies (specific, super shifted and non-specific (NS) binding complexes are indicated by arrows). (D) ChIp detection of CREB1, cjun, JunD and ATF1 proteins at the CRE/AP-1-like site (-153) region of the endogenous Atx promoter in SK-N-BE and SH-SY5Y cells. Input material (Input) and pre-immune rat (ra) and mouse IgG (mo) controls are provided.

3.7. SP-1 stimulates and internally initiated SP3 represses Atx transcription

Transient SP-1 expression in drosophila SL2 cells [34] significantly increased −1197Atx promoter activity by 122 ± 22.3% ($p \leqslant 0.001$, $n = 18$) but did not stimulate transcription from the mutated GAbox construct −1197GAmAtx (Fig. 6A). Transient expression of internally initiated SP-3 (pCMV4-spM2), an 80 kDa SP-3 isoform that arises from translational initiation within the SP-3 trans-activation domain, binds SP-1 binding sites and represses SP-1/SP-3-mediated transcription [34], did not stimulate transcription from either −1197Atx or 1197GAmAtx constructs and significantly reduced SP-1 stimulation of Atx reporter gene activity from 122 ± 22.3% to 55 ± 13% ($P \leqslant 0.05$, $n = 18$), upon co-transfection in SL2 cells (Fig. 6A). Neither SP-2 nor full-length SP-3 were evaluated due to expression problems (this study and 34). Transient expression of internally initiated SP-3 in SK-N-BE cells significantly inhibited Atx mRNA expression relative to empty vector transfected controls by 30 ± 5.2% ($P < 0.05$, $n = 4$), assessed by densitometric analysis of ethidium bromide stained gels (Fig. 7A).

3.8. C-Jun (AP-1) transactivates the Atx promoter

Transient c-Jun expression in SK-N-BE cells significantly increased −1197Atx but not mutated −1197CRE/AP-1-like-Atx reporter gene activity by 45 ± 13.3% ($P \leqslant 0.02$) compared to empty vector-transfected controls (Fig. 6B). Neither transient expression of dominant-negative kCREB [35] nor pre-incubation with dibutyrly cAMP Rp-isomer (100 μM) [36] reduced −1197Atx reporter gene activity in SK-N-BE cells (Fig 6B).

3.9. Curcumin abrogates Atx expression

Considering AP1 and SP transcription factor involvement in Atx expression, we evaluated the potential inhibitory effect of curcumin, a natural phenolic inhibitor of the thioredoxin-regulated transcription factors AP-1 and SP-1 [37–40]. Curcumin inhibited Atx relative to GAPDH mRNA expression in a dose dependent manner at concentrations $\geqslant 1$ μM in SK-N-BE cells and $\geqslant 10$ μM in SH-SY5Y cells, determined by densitometric analysis of ethidium bromide stained agarose gels and adjusted according to internal GAPDH control levels (Fig 7B). At the optimum non-toxic concentration of 10 μM, cur-

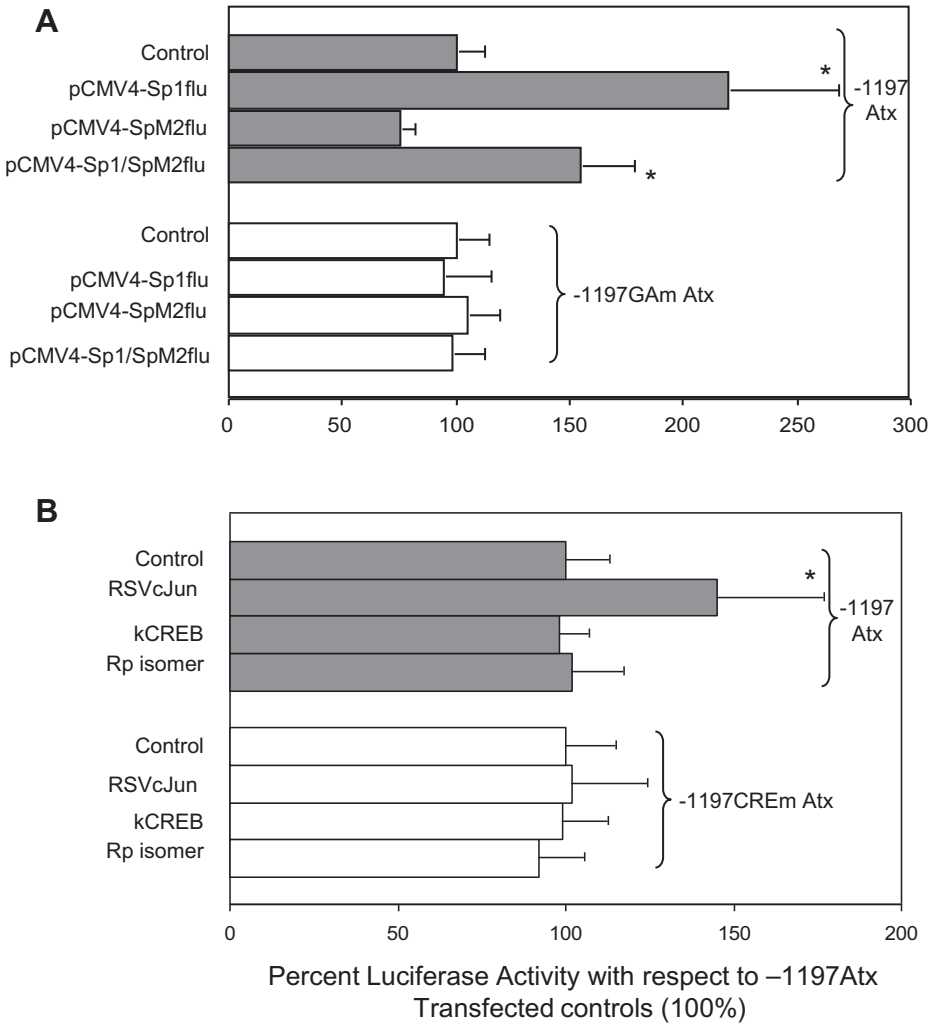

Fig. 6. C-jun and SP-1 activate the Atx promoter. (A) Histogram depicting differences in percentage luciferase activity in total extracts (100–200 μg) from SL2 cells co-transfected with −1197Atx or GAbox mutated −1197GAm reporter genes, with either empty vector, full length SP-1 cDNA (pCMV4-Sp1flu) or internal initiated SP-3 cDNA (pCMV4-SpM2flu). Results are expressed as mean (±s.e.) percentage luciferase activity with respect −1197Atx reporter gene and empty pCMV4 co-transfected controls (100%), in three independent experiments performed in triplicate. (B) Histogram depicting differences in percentage luciferase activity in total extracts (100–200 μg) from SK-N-BE cells transiently co-transfected with either −1197Atx or mutated CRE/AP-1-like-Atx (−1197CRE/AP1 m) reporter genes, together with either empty pRSV vector or RSV c-jun, dominant negative kCREB or following incubation with dibutyryl cAMP Rp-isomer (100 μM). Results are expressed as mean (±s.e.) percentage luciferase activity with respect to −1197Atx and empty pRSV co-transfected controls (100%), in three independent experiments performed in triplicate. All results were adjusted for differences in transfection efficiency obtained by β-galactosidase assay (* = significant difference).

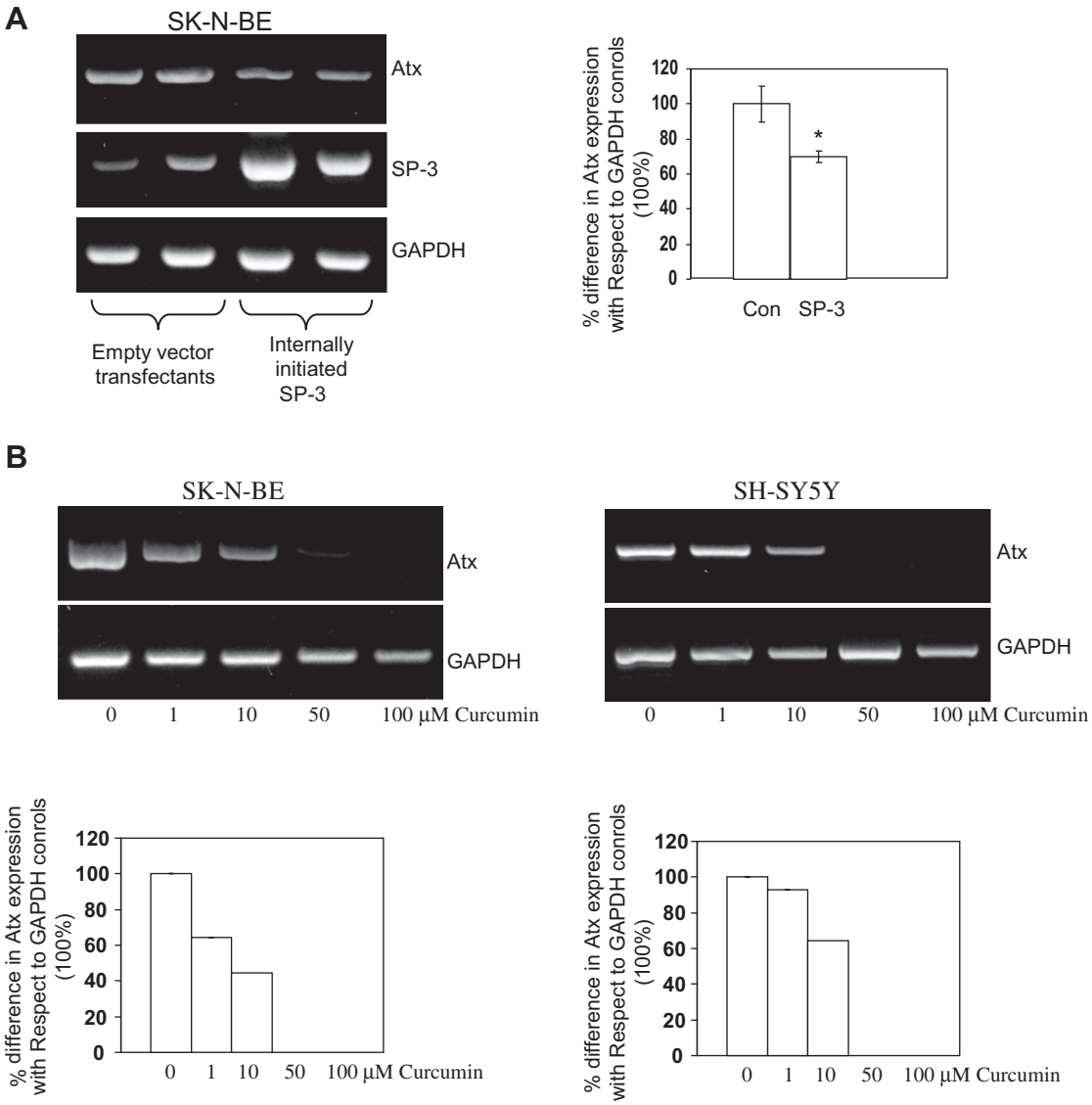

Fig. 7. Internally initiated SP-3 and curcumin inhibit Atx expression (A) Ethidium bromide-stained gels demonstrating inhibition of Atx relative to SP-3 and GAPDH mRNA expression in duplicate SH-SY5Y cultures transiently transfected with internally initiated SP-3 compared to empty vector controls. The adjacent histogram demonstrates the densitometric reduction in Atx relative to GAPDH mRNA expression associated with transient internally initiated SP-3 expression compared to controls, in 4 experiments (* = significant difference). (B) Ethidium bromide-stained gels demonstrating dose-dependent curcumin inhibition of Atx mRNA expression in SK-N-BE and SH-SY5Y cells following 24 h incubation at the concentrations indicated plus a histogram demonstrating densitometric quantification of Atx relative to GADH levels in the adjacent gel.

cumin reduced Atx relative to GAPDH mRNA expression by approximately 35% in SH-SY5Y cells and 55% in SK-N-BE cells and more toxic concentrations of 50 μm and 100 μm, which reduced SK-N-BE and SH-SY5Y viability by $\geqslant$50% within 24 h (data not shown), Atx expression was completely abrogated relative to GAPDH within the remaining viable adherent cell populations (Fig 7B).

4. Discussion

We characterise a novel transcriptional mechanism for constitutive Atx expression utilised by human Nmyc amplified SK-N-BE and non-Nmyc amplified SH-SY5Y NB cells. This mechanism is restricted to the first 285 bp of Atx promoter and mediated by AP1 and SP transcription factors acting through a CRE/AP-1-like element at position −142 to −149 and a GAbox at position −227 to −235, respectively. This constitutive mechanism is partially repressed by internally initiated SP-3 and can be completely abrogated by the natural phenol curcumin.

The similar level of constitutive Atx mRNA and protein expressed by Nmyc amplified SK-N-BE and non-Nmyc amplified SH-SY5Y NB cells, combined with the close similarity exhibited by both cell lines in in vitro footprint, EMSA, ChIp and Atx promoter reporter gene assays, suggests an identical transcriptional mechanism restricted to the initial 285 bp of the *Atx* promoter. Within this region, identical Atx promoter sequences were protected by nuclear extracts from both cell lines. The first, bases −155 to −137 (5′-*CCTGTGATGTAATCAAG*CT-3′), contains a putative CRE/AP1-like element, and the second, bases −238 to −207 (5′-*TTAGGGGAGGGACCTGTAAG GGGCGGGGATAA*-3′), contains a GAbox and a GCbox. A function for the CRE/AP1-like element and GAbox but not for putative GCbox, GATA or myc elements within this region [20] was confirmed by deletion and point mutation of these sites. Furthermore, simultaneous CRE/AP-1-like and a GAbox mutation abrogated Atx reporter gene activity in both cell lines, confirming an absolute requirement for both elements for full reporter gene activity in both cell lines. We found no evidence for involvement of the 33 bp region (bases −287 to −254) reported

to confer Atx promoter activity to SMS-KAN NB cells [20], suggesting that more than one mechanism for constitutive Atx transcription may characterise NB. We also exclude a potential function for the NFAT elements involved in integrin-mediated Atx transcription in human breast cancer cells [25].

AP-1 transcription factor [41] involvement in Atx transcription, acting through the CRE/AP-1-like element (−142 to −149), was supported by the identification of cjun, JunD and cfos proteins in specific CRE/AP-1-like site-binding complexes by EMSA and by ChIp detection of cjun and JunD at the endogenous Atx promoter, in both cell lines. Furthermore, transient c-Jun expression stimulated Atx reporter gene activity in SK-N-BE cells through the intact but not mutated CRE/AP-1-like element. These data help to explain v-Jun-induced Atx expression in transformation of chick embryo fibroblasts [27] and Epstein-Barr induced Atx expression in Hodgkin lymphoma cells considered potentially to involve AP-1 [15]. CREB-1 and ATF-1 transcription factors were also detected in specific CRE/AP-1-like (−153) site-binding complexes. However, neither transient dominant-negative kCREB transfection [35] nor pre-incubation with the CREB inhibitor cAMP Rp isomer [36] reduced Atx reporter gene activity, suggesting a CREB-independent transcriptional mechanism.

SP transcription factor involvement in Atx transcription, acting through the GAbox (−227 to −235), was supported by the identification of SP-1, 2 and 3 proteins in specific GAbox binding complexes in nuclear extracts by EMSA and by ChIp detection of same proteins at endogenous Atx promoter. Furthermore, transient SP-1 expression stimulated Atx reporter gene activity in non-SP expressing SL2 drosophila cells [34] through the intact but not mutated GAbox. In contrast, internally initiated SP-3, which represses SP1/3-mediated gene transcription [34,42], did not stimulate Atx promoter activity but significantly reduced SP-1 stimulation of Atx promoter activity in SL2 cells and, upon transient transfection, also inhibited Atx mRNA expression in SK-N-BE and SH-SY5Y cells, confirming a Atx transcription-repressing function for internally initiated SP-3 in these NB cell lines.

Considering AP1 and SP transcription factor involvement in Atx expression, we evaluated the potential inhibitory effect of curcumin, a natural phenolic inhibitor of thioredoxin-regulated AP-1 and SP-1 transcription factors [37–40]. Curcumin inhibited Atx mRNA expression at concentrations $\geqslant 1$ μM in SK-N-BE cells and $\geqslant 10$ μM and SH-SY5Y cells. At the optimum non-toxic concentration of 10 μM, curcumin inhibited Atx expression in both cell lines by 35–55% and at the more toxic concentrations of 50 μM and 100 μM completely abrogated Atx expression in the remaining viable adherent population of both cell lines.

We propose that the novel Atx transcriptional mechanism identified in this study, utilised by both Nmyc amplified and non-amplified NB, is mediated by AP1 and SP transcription factors acting through CRE/AP1-like (−142 to −149) and GAbox-elements (−227 to −235) and can be inhibited by internally initiated SP-3 and by the natural phenolic AP-1 and SP inhibitor curcumin.

Acknowledgements

Supported by AIRC, COFIN and Maugeri Foundation.

Appendix A. Supplementary data

Supplementary data associated with this article can be found, in the online version, at http://dx.doi.org/10.1016/j.febslet.2012.08.026.

References

[1] Stracke, M.L., Krutzsch, H.C., Unsworth, E.J., Arestad, A., Cioce, V., Schiffman, E. and Liotta, L.A. (1992) Identification, purification, and partial sequence analysis of Autotaxin, a novel motility-stimulating protein. J. Biol. Chem. 267, 2524–2529.
[2] Stracke, M.L., Clair, T. and Liotta, L.A. (1997) Autotaxin, tumor motility-stimulating exophosphodiesterase. Adv. Enzyme Regul. 3, 135–144.
[3] Clair, T., Lee, H.Y., Liotta, L.A. and Stracke, M.L. (1997) Autotaxin is an exoenzyme possessing 5′-nucleotide phosphodiesterase/ATP pyrophosphatase and ATPase activities. J. Biol. Chem. 272, 996–1001.
[4] Umezu-Goto, M., Kishi, Y., Taira, A., Hama, K., Dohmae, N., Takio, K., Yamori, T., Mills, G.B., Inoue, K., Aoki, J. and Arai, H. (2002) Autotaxin has lysophospholipase D activity leading to tumor cell growth and motility by lysophosphatidic acid production. J. Cell Biol. 158, 227–233.
[5] Liu, S., Murph, M., Panupinthu, N. and Mills, G.B. (2009) ATX-LPA receptor axis in inflammation and cancer. Cell Cycle 8, 3695–3701.
[6] Houben, A.J. and Moolenaar, W.H. (2011) Autotaxin and LPA receptor signalling in cancer. Cancer Metastasis Rev. 30, 557–565.
[7] van Leeuwen, F.N., Giepmans, B.N., van Meeteren, L.A. and Moolenaar, W.H. (2003) Lysophosphatidic acid: mitogen and motility factor. Biochem. Soc. Trans. 31, 1209–1212.
[8] Nam, S.W., Clair, T., Campo, C.K., Lee, H.Y., Liotta, L.A. and Stracke, M.L. (2000) Autotaxin (ATX), a potent tumor motogen, augments invasive and metastatic potential of ras-transformed cells. Oncogene 19, 241–247.
[9] Nam, S.W., Clair, T., Kim, Y.S., McMarlin, A., Schiffmann, E., Liotta, L.A. and Stracke, M.L. (2001) Autotaxin (NPP-2), a metastasis-enhancing motogen, is an angiogenic factor. Cancer Res. 61, 6938–6944.
[10] Ptaszynska, M.M., Pendrak, M.L., Stracke, M.L. and Roberts, D.D. (2010) Autotaxin signaling via lysophosphatidic acid receptors contributes to vascular endothelial growth factor-induced endothelial cell migration. Mol. Cancer Res. 8, 309–321.
[11] David, M., Wannecq, E., Descotes, F., Jansen, S., Deux, B., Ribeiro, J., Serre, C.M., Grès, S., Bendriss-Vermare, N., Bollen, M., Saez, S., Aoki, J., Saulnier-Blanche, J.S., Clézardin, P. and Peryuchaud, O. (2010) Cancer cell expression of autotaxin controls bone metastasis formation in mouse through lysophosphatidic acid-dependent activation of osteoclasts. PLoS One 5, e9741.
[12] Liu, S., Umezu-Goto, M., Murph, M., Lu, Y., Liu, W., Zhang, F., Yu, S., Stephens, L.C., Cui, X., Murrow, G., Coombes, K., Muller, W., Hung, M.C., Perou, C.M., Lee, A.V., Fang, X. and Mills, G.B. (2009) Expression of autotaxin and lysophosphatidic acid receptors increases mammary tumorigenesis, invasion and metastases. Cancer Cell 15, 539–550.
[13] Zhang, G., Zhao, Z., Xu, S., Ni, L. and Wang, X. (1999) Expression of autotaxin mRNA in human hepatocellular carcinoma. Chin. Med. J. (Engl.) 112, 330–332.
[14] Yang, Y., Mou, Lj., Liu, N. and Tsao, M.S. (1999) Autotaxin expression in non-small-cell lung cancer. Am. J. Respir. Cell Mol. Biol. 21, 216–222.
[15] Baumforth, K.R., Flavell, J.R., Reynolds, G.M., Davies, G., Pettit, T.R., Wei, W., Morgan, S., Stankovic, T., Kishi, Y., Arai, H., Nowakova, M., Pratt, G., Aoki, J., Wakelam, M.J., Young, L.S. and Murrey, P.G. (2005) Induction of autotaxin by the Epstein-Barr virus promotes the growth and survival of Hodgkin lymphoma cells. Blood 106, 2138–2146.
[16] Kishi, Y., Okudaira, S., Tanaka, M., Hama, K., Shida, D., Kitayama, J., Yamori, T., Aoki, J., Fujimaki, T. and Arai, H. (2006) Autotaxin is overexpressed in glioblastoma multiforme and contributes to cell motility of glioblastoma by converting lysophosphatidylcholine to lysophosphatidic acid. J. Biol. Chem. 281, 17492–17500.
[17] Kehlen, A., Englert, N., Seifert, A., Klonisch, T., Dralle, H., Langner, J. and Hoang-Vu, C. (2004) Expression, regulation and function of autotaxin in thyroid carcinomas. Int. J. Cancer 109, 833–838.
[18] Vidot, S., Witham, J., Agarwal, R., Greenhough, S., Bamrah, H.S., Tigyi, G.J., Kaye, S.B. and Richardson, A. (2010) Autotaxin delays apoptosis induced by carboplatin in ovarian cancer cells. Cell Signal. 22, 926–935.
[19] Stassar, M.J., Devitt, G., Brosius, M., Rinnab, L., Prang, J., Schradin, T., Simon, J., Petersen, S., Kopp-Schneider, A. and Zöller, M. (2001) Identification of human renal cell carcinoma associated genes by suppression subtractive hybridization. Br. J. Cancer 85, 1372–1382.
[20] Kawagoe, H., Stracke, M.L., Nakamura, H. and Sano, K. (1997) Expression and transcriptional regulation of the PD-I alpha/autotaxin gene in neuroblastoma. Cancer Res. 57, 2516–2521.
[21] Pahlman, S. and Hedborg, F. (2000) Development of the Neural Crest and Sympathetic Nervous System in: Neuroblastoma (Brodeur, G.M., Sawada, T., Tsuchida, Y. and Voute, P.A., Eds.), pp. 9–19, Elsevier Science BV.
[22] Brodeur, G.M. and Maris, J.M. (2006) Neuroblastoma in: Principles and Practice of Pediatric Oncology (Pizzo, P.A. and Poplack, D.G., Eds.), pp. 933–970, Lippincott, Williams and Wilkinson.
[23] Kawagoe, H., Soma, O., Goji, J., Nishimura, N., Narita, M., Inazawa, J., Nakamura, H. and Sano, K. (1995) Molecular cloning and chromosomal assignment of the human brain-type phosphodiesterase I/nucleotide pyrophosphatase gene (PDNP2). Genomics 30, 380–384.
[24] Dufner-Beattie, J., Lemons, R.S. and Thorburn, A. (2001) Retinoic acid-induced expression of Autotaxin in N-myc-amplified neuroblastoma cells. Mol. Carcinog. 30, 181–189.
[25] Chen, M. and O'Connor, K.L. (2005) Integrin alpha6beta4 promotes expression of autotaxin/ENPP2 autocrine motility factor in breast carcinoma cells. Oncogene 24, 5125–5130.
[26] Li, S., Wang, B., Xu, J. and Zhang, J. (2011) Autotaxin is induced by TSA through HDAC3 and HDAC7 inhibits and antagonizes the TSA-induced cell apoptosis. Mol. Cancer., 10–18.
[27] Black, E.J., Clair, T., Delrow, J., Neiman, P. and Gillespie, D.A. (2004) Microarray analysis identifies Autotaxin, a tumour cell motility and angiogenic factor

with lysophospholipase D activity, as a specific target of cell transformation by v-Jun. Oncogene 23, 2357–2366.
[28] Williams, T.M., Williams, M.E., Kuick, R., Misek, D., McDonagh, K., Hanash, S. and Innis, J.W. (2005) Candidate downstream regulated genes of HOX group 13 transcription factors with and without monomeric DNA binding capability. Dev. Biol. 279, 462–480.
[29] Dignam, J.D., Martin, P., Shastry, B.S. and Roeder, R.G. (1983) Eukaryotic gene transcription with purified components. Methods Enzymol. 101, 582–598.
[30] Farina, A.R., Tacconelli, A., Vacca, A., Maroder, M., Gulino, A. and Mackay, A.R. (1999) Transcriptional up-regulation of matrix metalloproteinase-9 expression during spontaneous epithelial to neuroblast phenotype conversion by SK-N-SH neuroblastoma cells, involved in enhanced invasivity, depends upon GT-box and nuclear factor kappa B elements. Cell Growth Differ. 10, 353–367.
[31] Cappabianca, L., Farina, A.R., Tacconelli, A., Gulino, A., Mantovani, R. and Mackay, A.R. (2003) Reconstitution of TIMP-2 expression in SH-SY5Y neuroblastoma cells by 5-azacytidine is mediated transcriptionally by NF-Y through an inverted CCAAT site. Exp. Cell Res. 286, 209–218.
[32] Flavin, M., Cappabianca, L., Kress, C., Thomassin, H. and Grange, T. (2004) Nature of the accessible chromatin at a glucocorticoid-responsive enhancer. Mol. Cell Biol. 24, 7891–7901.
[33] Burnette, W.G. (1981) "Western blotting": electrophoretic transfer of proteins from sodium dodecyl sulphate polyacrylamide gels to unmodified nitrocellulose and radiographic detection with antibody and radioiodinated protein. Anal. Biochem. 112, 195–203.
[34] Kennett, S.B., Udvadia, A.J. and Horowitz, J.M. (1997) Sp3 encodes multiple proteins that differ in their capacity to stimulate or repress transcription. Nucleic Acids Res. 25, 3110–3117.
[35] Walton, K.M., Rehfuss, R.P., Chrivia, J.C., Lochner, J.E. and Goodman, R.H. (1992) A dominant repressor of cyclic adenosine 3′, 5′-monophosphate (cAMP)-regulated enhancer-binding protein activity inhibits the cAMP-mediated induction of the somatostatin promoter in vivo. Mol. Endocrinol. 6, 647–655.
[36] Dragland-Meserve, C.J., Rothermel, J.D., Houlihan, M.J. and Botelho, L.H. (1985) Inhibition of cyclic AMP-dependent protein kinase-induced changes in the kinetic properties of hepatic pyruvate kinase by the specific cyclic AMP antagonist, the (Rp)-diastereomer of adenosine cyclic 3′,5′-phosphorothioate. J. Cyclic Nucleotide Protein Phosphor. Res. 10, 371–382.
[37] Singh, D.J. and Misra, K. (2009) Curcuminoids as inhibitors of thioredoxin reductase: a receptor based pharmacophore study with distance mapping of the active site. Bioinformation 4, 187–192.
[38] Dhandapani, K.M., Mahesh, V.B. and Brann, D.W. (2007) Curcumin suppresses growth and chemo resistance of human glioblastoma cells via AP-1 and NFkB transcription factors. J. Neurochem. 102, 522–538.
[39] Han, S., Keum, Y.S., Seo, H.J. and Suhr, Y.J. (2002) Curcumin suppresses activation of NFkB and AP-1 induced by phorbol ester in cultured human promyelocytic leukemia cells. J. Biochem. Mol. Biol. 35, 337–342.
[40] Kang, Q. and Chen, A. (2009) Curcumin inhibits srebp-2 expression in activated hepatic stellate cells in vitro by reducing the activity of specificity protein-1. Endocrinology 150, 5384–5394.
[41] Eferl, R. and Wagner, E.F. (2003) AP-1: a double-edged sword in tumorigenesis. Nat. Rev. Cancer 3, 859–868.
[42] Bakovic, M., Waite, K.A. and Vance, D.E. (2000) Functional significance of Sp1, Sp2, and Sp3 transcription factors in regulation of the murine CTP: phosphocholine cytidylyltransferase alpha promoter. J. Lipid Res. 41, 583–594.